
Chapter 2

**Exploring wild-type rat
glucocerebrosidase: Insights into
chaperone interactions and
mechanism through *in silico* and *in
vitro* studies**

2 Introduction

New treatment strategy for Parkinson's disease (PD) by stabilization of Glucocerebrosidase (GCase) enzyme by chaperones is of particular interest (Maegawa, Tropak et al. 2009, Dhanve, Aggarwal et al. 2023). However, it is worth noting that the current research primarily relies on genetic models, which are applicable to only a small percentage of PD cases. These genetic cases account for approximately 3-5% of all PD, while the majority, around 90-95%, are classified as sporadic cases (Beavan and Schapira 2013, Yang, Wu et al. 2023). Unfortunately, the lack of an established non-genetic model poses a challenge when it comes to validating GCase activity. Without a reliable non-genetic model, it is difficult to fully investigate and comprehend the significance of GCase in sporadic PD cases. This limitation underscores the need for further research and the development of non-genetic models that can accurately replicate the characteristics of sporadic PD and allow for the evaluation of GCase function.

Our laboratory introduced the validation of a non-genetic model of PD induced by 6-OHDA to evaluate the compounds that target GCase activity, with the support of AMB as a chaperone (Mishra, Chandravanshi et al. 2018). The Lawson Health Research Institute is developing chaperone (Ambroxol, AMB) as the first disease-modifying therapy for PD with dementia (NCT02914366) (Silveira, MacKinley et al. 2019). Many reports support that AMB increases wild-type glucocerebrosidase (GCase) activity and decreases the levels of α -synuclein aggregation in cell lines, preclinical and clinical PD models (Gegg, Burke et al. 2012, Magalhaes, Gegg et al. 2018, Kopytova, Rychkov et al. 2021). Studies in our lab on sub-chronic administration of AMB have shown a disease-modifying effect by increasing wild-type GCase activity in the rat-PD model (Mishra and Krishnamurthy 2020). In a wild-type rat PD model, another study of our lab showed that 6-Hydroxydopamine hydrochloride (6-OHDA, neurotoxin)-induced reduction in GCase

activity is enhanced by AMB (Mishra, Chandravanshi et al. 2018). As wild-type rat is a widely used model for the PD at the initial phases of drug discovery and chaperone is developing as an anti-PD drug; however, its *in silico* and *in vitro* screening of chaperon on the rat GCCase (rGCCase) is still unavailable. The absence of disease-modifying chaperones during both the preclinical and clinical trial phases might be attributed to this factor. Consequently, it becomes imperative to develop efficient screening techniques that can assess the mechanisms and structural stability of rGCCase-chaperone interactions.

GCCase (Enzyme classification, EC: 3.2.1.45) is a GBA1 encoded lysosomal acid glycoside hydrolase (GH) of family 30 that belongs to a class of clan GH-A (Cairns, Mahong et al. 2015). The synthesis and folding of the GCCase enzymes are completed in the endoplasmic reticulum (ER, neutral pH: 7.0). Following their correct folding, they are trafficked to lysosomes, where they metabolize the substrate glucocerebrosides (GC) into glucose and ceramide. A human matured GCCase comprises of 497 amino acids with around 60 kDa molecular weight. The crystal structural topology of human GCCase (hGCCase) displays three domains, *viz.*: domain I (residues 1-27 and 383-414); domain II (residues 30-75 and 431-497); and domain III (residues 76-381 and 416-430). The active site cavity is in domain III and consists of an atypical $(\alpha/\beta)_8$ triosephosphate isomerase (TIM) barrel motif. Further, the active site cavity of hGCCase is comprised of ARG 120, ASP 127, PHE 128, TRP 179, ASN 234, GLU 235, TYR 244, PHE 246, GLN 247, GLU 340, CYS 342, SER 345, TRP 381, ASN 396, PHE 397 and VAL 398, which helps in ligand recognition, interaction, holding and their stabilization. Other than these residues, several loops (loop 1; 311-319, loop 2; 342-354, loop 3; 394-399, loop 4; 237-248 and, loop 5; 283-288) are arranged in and around the cavity. All are pH-sensitive, highly flexible or movable, and adopt distinct configurations at different pH environments (neutral to acidic). These configurations extensively affect the shape of the active site

where the ligands (chaperones) are accommodated (Smith, Mullin et al. 2017, Nakagome, Kato et al. 2018).

Chaperones function as enzyme inhibitors that are pH-dependent, specifically designed to exhibit a higher binding capacity to misfolded GCCase at the pH of the endoplasmic reticulum (ER) (neutral: 7.0) (Yu, Sawkar et al. 2007). Their purpose is to stabilize the misfolded GCCase by facilitating its correct folding, preventing its degradation within the ER. They may also tie to a wild-type rGCCase and stabilize it so that it does not get misfolded. Once the correct folding and stabilization are achieved, these chaperones enable the enzymes to traffic through the ER towards the lysosomes (acidic pH: 5.0 - 4.5). At this stage, the GCCase-chaperone complex dissociates due to the acidic pH, allowing the enzymes, depending on their residual activity, to cleave their respective substrates (Lieberman, D'aquino et al. 2009, Trapero and Llebaria 2011).

Unfortunately, the commercial rGCCase and its 3D structure are unavailable. Thus, in this study, *in silico* and *in vitro* evaluations of a chaperon on rGCCase were established. For this motive, we have shifted our primary interest to isolate ER fractions from rat brains and used them as a source of rGCCase. The reason for choosing ER fractions instead of lysosomal fractions lies in the fact that chaperones bind best with the GCCase in the ER than the lysosomes (Yu, Sawkar et al. 2007, Lieberman, D'aquino et al. 2009). Apart from this, trafficking of GCCase or GCCase-chaperone complex occurs only from ER to lysosomes (Trapero, Gonzalez-Bulnes et al. 2012). The selection of ER fraction for rGCCase activity was also supported from the pilot study done in our lab, where no difference in the activity of rGCCase was observed at the acidic pH of lysosome and the acidified ER fractions (**Figure 2.1 in Appendices**). AMB is a well-known GCCase chaperone (Bendikov-Bar, Maor et al. 2013); thus, used it to validate the model. pH-dependent 3D-structures of rGCCase were constructed by homology modeling using

SWISS-model and validated by Ramachandran-plots. pH-dependent molecular docking and molecular dynamics (MD) simulation study was carried out to analyze the effect of pHs on the nature of GCCase-chaperone interactions, mechanism, and structural stability. *In vitro*, pH-dependent enzyme activity, binding affinity, and enzyme inhibition mechanism were done. Further, the structural stability of rGCCase was confirmed by a thermal denaturation assay.

Therefore, our objective was to develop a homology model for rGCCase and evaluate the nature of its interaction with the chaperon by using docking, molecular dynamics, and *in vitro* mechanistic studies. This research will provides a framework for developing and screening chaperones during the early stages of drug discovery in order to alleviate PD. The experimental design is outlined in the Figure 2.1. ~~Error! Reference source not found., which provides a representation of the planned methodology.~~

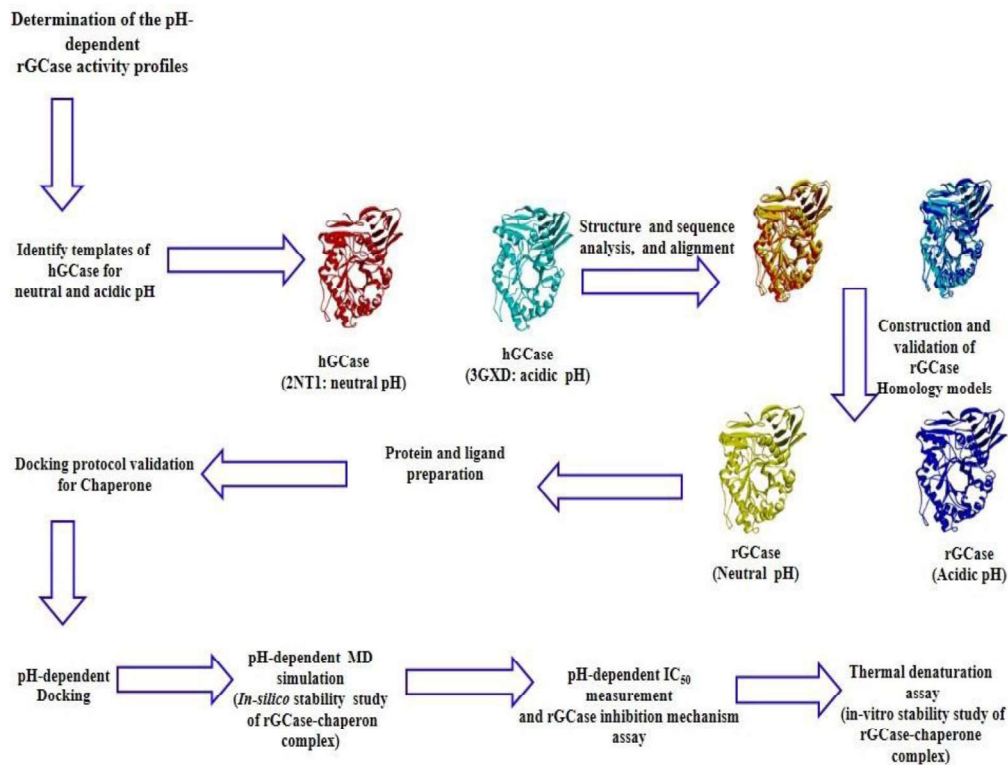


Figure 2.1 Schematics work flow of the objective 2

2.1 Material and method

2.1.1 Material

AMB (GCase chaperone) was obtained as a gift sample from Meenaxi Pharma Pvt. Ltd. (Delhi, India). Taurodeoxycholic acid sodium salt (TDC) was procured from Cayman chemicals. 4-methylumbelliferyl- β -D-glucopyranoside (4-MUG), 4-methylumbelliferone (4-MU), and Triton X-100 were acquired from Sigma-Aldrich (St. Louis, MO, USA). Citric acid, sodium phosphate dibasic, and Tris-HCL were supplied by Hi-media (Mumbai). All other reagents used were of analytical grade, and triple distilled water was used to prepare the reagents.

2.2 Methods

2.2.1 Determination of the pH-dependent rGCase activity profiles

In order to determine the optimal pH condition for rGCase activity, we conducted pH-dependent enzymatic activity assays using a fluorometric method (Page 215-218 in appendices). The reaction was carried out in a final volume of 220 μ l, using McIlvaine buffer (100 mM citric acid, 200 mM sodium phosphate buffer, 0.2% TDC, and 0.1% Triton X-100) with pH ranging from 7.0 to 4.0. The reaction mixture included 10 μ g of rGCase (20 μ l, 0.5 μ g of protein/ μ l), 100 μ l of McIlvaine buffer at varying pH levels, and 25 μ l of the substrate 4-MUG (final concentration 2.5 mM in McIlvaine buffer, pH 7.0 - 4.0). The mixtures were incubated for 30 minutes, and the reaction was stopped by adding 75 μ l of 200 mM glycine/sodium hydroxide buffer (pH 10.7). Fluorescence measurements were taken using a Synergy HTX multi-mode reader (BioTek, USA) at an excitation-emission wavelength of 355:460 nm. Obtained Fluorescence was converted into a concentration of fluorescent product (4-MU) using the product standard curve

(Graph Pad Prism 5.1 Software, Inc.), and interpolated values were used to calculate the enzyme activity (nmoles/hr/mg protein). The standard curve of the same pH conditions as that of the samples was used to calculate the GCCase activity (Trapero, Gonzalez-Bulnes et al. 2012, Berger, Perkins et al. 2015).

2.2.2 Construction of rGCCase homology models and their validation

2.2.2.1 Sequence Retrieval

The amino acid sequence of the rGCCase target protein for *Rattus norvegicus* was obtained in a FASTA file format using UniProtKB database (www.uniprot.org). The UniProtKB ID of the obtained sequence is B2RYC9 (B2RYC9_RAT).

2.2.2.2 Homology modeling

Basic Local Alignment Search Tool (BLAST) and UCSF chimera were utilized for sequence alignment after the superimposition of both proteins. SWISS-MODEL (<https://swissmodel.expasy.org/>) tool was used to develop homology models for the rGCCase. The human GCCase protein Data Bank ID (PDB: 2NT1) was utilized as a template for the target protein (rGCCase), which was obtained from the www.rcsb.org web site. PROCHECK ([https:// servicesn.mbi.ucla.edu/ PROCHECK](https://servicesn.mbi.ucla.edu/PROCHECK)), RAMPAGE (<http://mordred.bioc.cam.ac.uk/~rapper/rampage.php>), VARIFY-3D ([https:// servicesn.mbi.ucla.edu/varify_3D](https://servicesn.mbi.ucla.edu/varify_3D)), and EERAT ([https:// servicesn.mbi.ucla.edu/EERAT](https://servicesn.mbi.ucla.edu/EERAT)) web servers were applied to evaluate the quality of the model. Chimera was used for visual examination. The modeling protocol has been elaborated in the previous studies (Ganeshpurkar, Kumar et al. 2018, Ganeshpurkar, Singh et al. 2022).

2.2.3 *In silico* study

2.2.3.1 Protein and ligand preparation, and grid generation

To facilitate the molecular docking analysis, the structurally refined rGCCase protein PDB files were transformed into PDBQT files using AutoDock Tools 1.5.6. Meanwhile, the ligand structure (AMB) was created using ChemDraw 16, followed by energy minimization via the MMFF94 force field using Chem3D. The resulting ligand structure was saved as a PDB file and subsequently converted to PDBQT format using the ligand preparation module of AutoDock 1.5.6 tools. Grid maps were calculated by Autogrid 4.0, which helps to identify the contact energies of several atoms present in the ligand (Ganeshpurkar, Kumar et al. 2018, Ganeshpurkar, Singh et al. 2022).

2.2.3.2 Docking

The docking was consecutively performed using AutoDock-4.2.6 employing Lamarckian Genetic Algorithm (LGA). The LGA helped to find out the best conformers or binding modes, and a maximum limit of the conformers was set at 10. Discovery Studio Visualizer 2019 was used to analyze the docked structures for getting the binding interactions [20-22]. The docking protocol was validated using previously reported method (Jana, Ganeshpurkar et al. 2018, Shukla, Shukla et al. 2018).

2.2.3.3 MD simulation

MD is another computational biology-based simulation approach that is often used to understand the dynamics of biological macromolecules as a function of time and results in their conformational changes in a particular environment in which it resides. MD was performed for rGCCase, and rGCCase-AMB complex through Desmond v2.2, Schrodinger 2015-1 tool. The protein-ligand complex was soaked in a TIP3P (Transferable Intermolecular Potential with 3 Points) hydrated cubic box. The cutoff distance was fixed at 12 Å. The system was exposed to a series of stages before the MD run, such as energy

minimization followed by heating and density equilibration. The time was fixed for the 50 ns at temperature 310.15 K as an NPT ensemble (Jana, Ganeshpurkar et al. 2018, Ganeshpurkar, Singh et al. 2020).

2.2.4 *In vitro* studies

2.2.4.1 Determination of rGCCase activity profiles in the presence of chaperone

The assay was conducted using 220 μ l of McIlvaine buffer at various pH values, including 7.0, 5.5, 5.2, 4.5, and 4.0. To determine the IC₅₀ values, 10 μ g of rGCCase (20 μ l, 0.5 μ g of protein/ μ l) was pre-incubated with seven concentrations of AMB ranging from 0 to 1500 μ M for 30 minutes on ice. Subsequently, 95 μ l of McIlvaine buffer at the respective pH values mentioned above were added to each well, followed by the addition of 25 μ l of the substrate 4-MUG. The preparation of McIlvaine buffer, substrate, and other assay steps remained consistent with those mentioned in **section 2.2.1**. The IC₅₀ values were calculated by plotting the logarithm of inhibitor concentrations (log [I]) against the percentage of fluorescence signals. The control samples without the test drug were set as 100% fluorescence signal for comparison (Trapero, Gonzalez-Bulnes et al. 2012, Berger, Perkins et al. 2015).

2.2.4.2 pH-dependent residual activity assay

0.5-2.0-folds concentration near to pH 7.0 IC₅₀ value of AMB was used for this study (concentrations detailed in **Figure 2.11**). They were incubated with rGCCase at various pHs, i.e., pH 7.0, 5.5, 5.2, 5.0, and 4.5, before the addition of substrate. The protocol was followed as described in section 2.4.1. Simultaneously, control experiments were performed at each pH by removing the AMB with its vehicle and taking it as 100 % rGCCase activity (Trapero, Gonzalez-Bulnes et al. 2012, Berger, Perkins et al. 2015, Karatas, Dogan et al. 2020). Percentage (%) residual enzymatic activity after inhibition

by AMB for each pH relative to their respective control was assessed by the formula given below

$$\text{Residual enzyme activity} = 100 - \left[\frac{F_0 - F_i}{F_0} \right] \times 100$$

where,

F_i = Fluorescence obtained in the presence of AMB

F_0 = Fluorescence corresponding to the same pH of control

2.2.4.3 pH-dependent enzyme kinetics assay

pH-dependent kinetic studies were performed to assess the pH-dependent rGCCase inhibition mechanism by AMB. Six (0.5 mM – 16 mM) substrate concentrations were taken for the enzyme kinetics study. Each substrate concentration was incubated with the rGCCase in the presence and absence of different concentrations of AMB. Samples without AMB were assumed to be showing 100 % rGCCase activity. The AMB concentration chosen was 0.5 X IC_{50} , 1 X IC_{50} , and 2 X IC_{50} of pH 7.0, 5.5 and 5.2 each (concentrations detailed shown in **Figure 2.12**). The Fluorescence was taken at 2 min intervals for 10 min. The standard curve of 4-MU was used to quantify the amount of product formation during the 10 min time frame, and their slope was used to measure the velocity of enzyme reaction. Michaelis–Menten constant (K_m) and maximum reaction rate (V_{max}) values were extracted by Michaelis-Menten non-linear regression graph (velocity in nmoles/h/mg protein *versus* substrate concentration) using software Graph Pad Prism 5.1. X-axis intercept ($-K_i$) of the Dixon plot (slope of the reciprocal plot of velocity plotted *versus* inhibitor concentration ($[I]$) used to extract the K_i values as previously described (Berger, Perkins et al. 2015, Shidore, Machhi et al. 2016, Gutti, Kumar et al. 2019).

2.2.4.4 *In vitro* thermal denaturation assay

To evaluate the chaperoning properties of AMB, a modified thermal heat-inactivation method was employed. Briefly, varying concentrations (0-100 μM) of AMB were added to two identical sets of plates, each containing 50 μl of rGCCase fractions (stock: 20 $\mu\text{g}/\mu\text{l}$). One set was kept on ice, while the other was subjected to denaturation by incubating at 48°C for over 60 minutes, followed by 5 minutes on ice. Both sets were then allowed to equilibrate at room temperature for an additional 10 minutes. To acidify the reaction mixtures, 3 volumes of McIlvaine buffer (100 mM citric acid, 200 mM sodium phosphate buffer, pH 4.5) were added to each well of both plates. Subsequently, 100 μl of the substrate (4 mM, final concentration) was added at different time points and incubated for an additional 15 minutes at 37°C. The enzyme reaction was terminated by adding glycine buffer (pH 10.6). The liberated 4-MU product was quantified as described earlier (excitation:emission; 355 nm:460 nm). Enzyme activity was reported relative to the unheated enzyme (Sawkar, Cheng et al. 2002, Goldin, Zheng et al. 2012).

2.2.5 Data analysis

All the experimental data analysis was performed using GraphPad Prism 5.1 and Microsoft Excel version 20. All datasets were expressed in the form of mean \pm standard deviation (SD), and triplicate samples were used. The statistical significance for pH-dependent effect on rGCCase activity was analyzed by one-way ANOVA followed by Tukey post-hoc test. Thermal denaturation assay and pH-dependent effect of chaperone on rGCCase activity (residual activity) were analyzed by two-way ANOVA followed by Bonferroni post-hoc test. Enzyme kinetics and other datasets were analyzed by Microsoft Excel version 20 and GraphPad Prism 5.1 using the mode of non-linear regression analysis. $p < 0.05$ was considered significant in the overall data analysis.

2.3 Result and discussion

2.3.1 Determination of the pH-dependent rGCCase activity profiles

The physiological functions of GCCase are intricately linked to pH conditions, as they are exposed to a wide range of pHs during their trafficking process, ranging from neutral (pH 7.0) to acidic (pH 5.0 - 4.5) environments. These pH levels play a crucial role in determining enzymatic conformation, structural stability, and catalytic activity (Smith, Mullin et al. 2017). To identify the optimal pH condition for achieving maximum enzyme activity, we evaluated a range of pH values from 7.0 to 4.0. The optimal pH required for maximum catalytic activity was found to be at pH 4.5 (pH of the lysosomal environment), which was ~ 3.5-fold higher than the enzymatic activity found at pH 7.0 (found in the ER) [Table 2.1]. These differences in the rGCCase enzymatic activity stipulated that the activity profile of rGCCase was sensitive to pHs due to either conformational changes or changes in protein flexibility. Also, studies carried out from different sources of GCCase have reported a pH-dependent GCCase activity profile showing optimal activity at the acidic pH in a range of 5.0 - 4.5 (Goldin, Zheng et al. 2012, Berger, Perkins et al. 2015).

Table 2.1 pH-dependent enzyme activity profiles of rGCCase

pH	Enzyme activity (nmoles/hr/mg protein)	Relative rGCCase activity (%)
pH 4.5	55.8 ± 7.6	100 ± 0.0
pH 7.0	15.7 ± 2.5	28.1 ± 3.7 ^a
pH 6.5	20.3 ± 2.1	36.4 ± 2.9 ^{a, b}
pH 5.5	31.1 ± 6.4	55.7 ± 9.6 ^{a, b, c}

Exploring wild-type rat glucocerebrosidase: Insights into chaperone interactions and mechanism through *in silico* and *in vitro* studies

pH 5.2	42.8 ± 8.6	76.7 ± 12.2 ^{a, b, c, d}
pH 5.0	46.3 ± 7.78	82.9 ± 10.4 ^{a, b, c, d}
pH 4.0	12.2 ± 2.4	21.8 ± 3.5 ^{a, c, d, e, f}

Rat Glucocerebrosidase (rGCCase) shows the maximum activity at pH 4.5, an optimal pH condition found in the lysosomes. This maximum enzyme activity of pH 4.5 was taken as 100 % to calculate the relative enzyme activity as depicted in the form of %. All values are expressed as mean ± SD of at three independent runs (n=3).^a p < 0.05 compared to pH 4.5, ^bp < 0.05 compared to pH 7.0, ^c p < 0.05 compared to pH 6.5, ^dp < 0.05 compared to pH 5.5 and ^e p < 0.05 compared to pH 5.2, ^f p < 0.05 compared to pH 5.0 [One-way ANOVA followed by Tukey test].

2.3.2 Construction of rGCCase homology models and their validation

As we found in our above study that the optimal lysosomal pH condition for rGCCase catalytic activity was pH 4.5, which was ~ 3.5-fold higher than the enzymatic activity seen at the ER pH 7.0. Therefore, there is a necessitates to study the structural changes in protein at both the pHs. Based on the above facts, we have constructed homology modeling at both pHs using PDB: 2NT1 (neutral pH) and PDB: 3GXD (acidic pH) of hGCCase in apo form as a template. Constructed homology models showed about 88% identity, 59% similarity, and 96% query cover (**Figure 2.2**) with hGCCase.

Exploring wild-type rat glucocerebrosidase: Insights into chaperone interactions and mechanism through *in silico* and *in vitro* studies

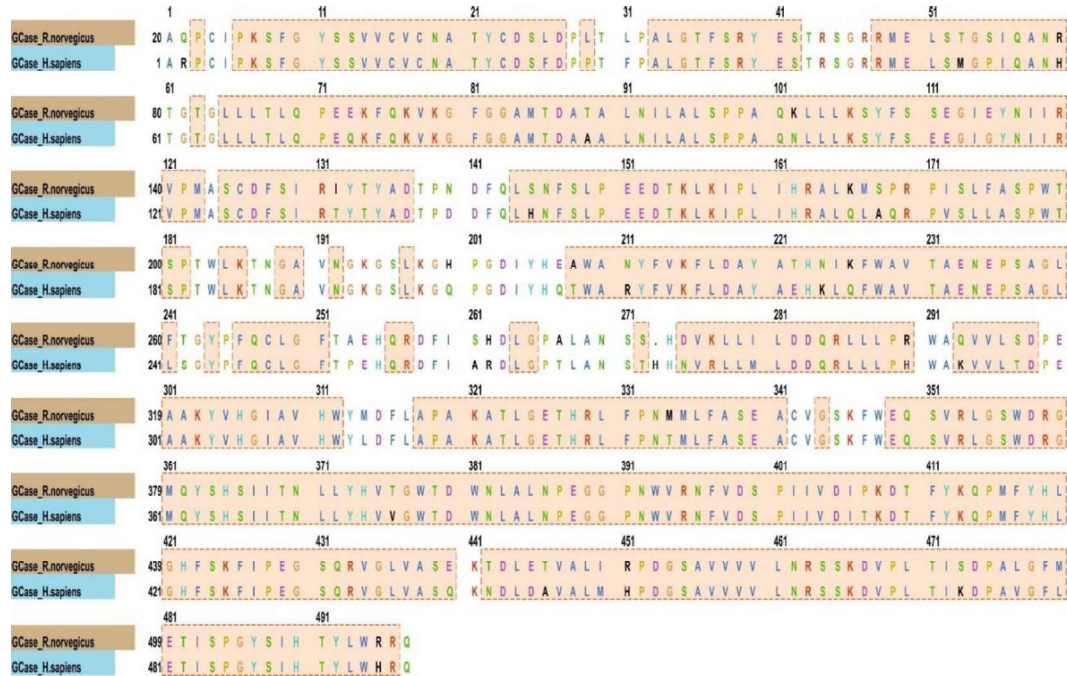


Figure 2.2 Sequence alignment between the template (hGCCase: human-Glucocerebrosidase, organism: Homo sapiens, PDB: 2NT1) and target (rGCCase: rat-Glucocerebrosidase, organism: Rattus norvegicus, Protein code: B2RYC9_RAT) protein.

Ramachandran plot analyzed by PROCHECK revealed the presence of most of the residues ($\leq 90\%$) in the favored regions and only a few ($\geq 0.5\%$) in the disallowed regions. However, RAMPAGE outcomes showed $\leq 94\%$ of rGCCase residues in the maximum preferred regions, while $\geq 1.0\%$ of the residues were in the outliers. These results validate the quality of the models. The GMQE value defined the model's accuracy, which was about 0.91 for both models, representing the model's proximity to the templates. The QMEAN estimates a global score for the models. The model's reliability score falls within the scale range from 0 to 1, and our models showed a value of 0.55 on the scale. The QMEAN Z-score uses the reference X-ray crystallography structures to estimate the model's quality. A score below -4.0 indicates models with low quality. QMEAN Z-score was found to be about -1.20 for both models. VARIFY-3D outcomes revealed that more

than 98% of the residues had an average 3D-1D score \geq of 0.2, which was higher than the cutoff limit of 80%. EERAT tool was used to identify the overall resolution of the proteins in which the values were more than 93.5 for both models showed high-resolution structures. Overall, the quality factors (PROCHECK, RAMPAGE, GMQE, QMEAN, QMEAN Z-score, VARIFY-3D, and EERAT) confirmed the correctness of the developed homology models (**Table 2.2 and Figure 2.3**) and is trustworthy for further docking and MD simulation experiments.

Table 2.2 Quality parameters of Ramachandran plots for the rGCase attained by PROCHECK RAMPAGE, VARIFY-3D and ERRAT

Method		rGCase_pH 7.0 (%)	rGCase_pH 4.5 (%)
PROCHECK	Residues most favored regions	9.2	90.8
	Residues additional allowed regions	9.6	7.9
	Residues generally allowed regions	0.0	0.7
	Residues disallowed regions	0.2	0.5
RAMPAGE	Most favored regions	94.5	95.5
	Outliers	0.9	0.7
VARIFY-3D	3D-ID score	97.6	98.9
ERRAT	Quality factor	93.9	94.5

A pairwise comparison of the amino acid sequences as well as the superimposition of two protein models resulted in identification of domains, loops, active site cavities, and conformational changes in the homology constructed at neutral and acidic pH (**Figure 2.4a-b**). The hGCCase and rGCCase have a multidomain structure with molecular weight around 59 kDa each. After careful analysis of superimposed proteins, we found that the domain I of the wild-type rGCCase extended from residues 20 - 46 and 401 - 432, corresponding to the domain I of hGCCase residues 1 - 27 and 383 - 414. While domain II from 49 - 94 and 450 - 515 corresponds to 30 - 75 and 431 - 497 residues of hGCCase domain II.

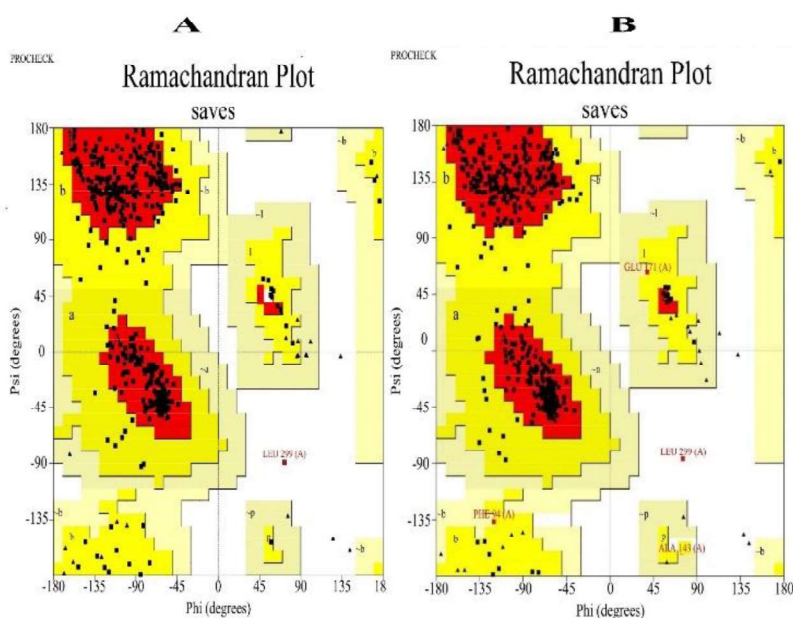


Figure 2.3 Ramachandran plots of the constructed rGCCase homology models at pH 7.0 (A) and 4.5 (B) are acquired by PROCHECK. A, B, and L denotes the residues in the most favored regions. Residues in the additional and generally allowed regions are shown by a, b, l, p and ~a, ~b, ~l, ~p, respectively.

Similarly, domain III, active site of the enzyme, was stretched out from 95 - 399 and 434 - 448 in rGCCase when compared to domain III of hGCCase, i.e., 76 - 381 and 416 - 430. GLU 254 and GLU 358 are the active catalytic residues of the rGCCase, which corresponds to hGCCase GLU 235 and GLU 340. Moreover, four main loops *viz.* loop 1; 329 - 337, loop 2; 360 - 373 and loop 3; 412 - 417, and loop 4; 256 - 267 were identified in rGCCase which were similar to hGCCase loop 1; 311 - 319, loop 2; 342 - 354, loop 3; 394 - 399, and loop 4; 237 - 248, respectively. A shift in loop 1 and loop 2 was detected in rGCCase at acidic pH while comparing it to the corresponding pH of hGCCase (**Figure 2.2 in Appendices**). However, when we superimposed rGCCase structures of neutral pH 7.0 on acidic pH 4.5, we have noticed a conformational change in loop 1 (from residues ASP 333 - ALA 336) and loop 2 (CYS 360) at acidic pH 4.5. These conformational changes in the active site loops could be the reason of the change in rGCCase enzymatic activity as observed in our above study.

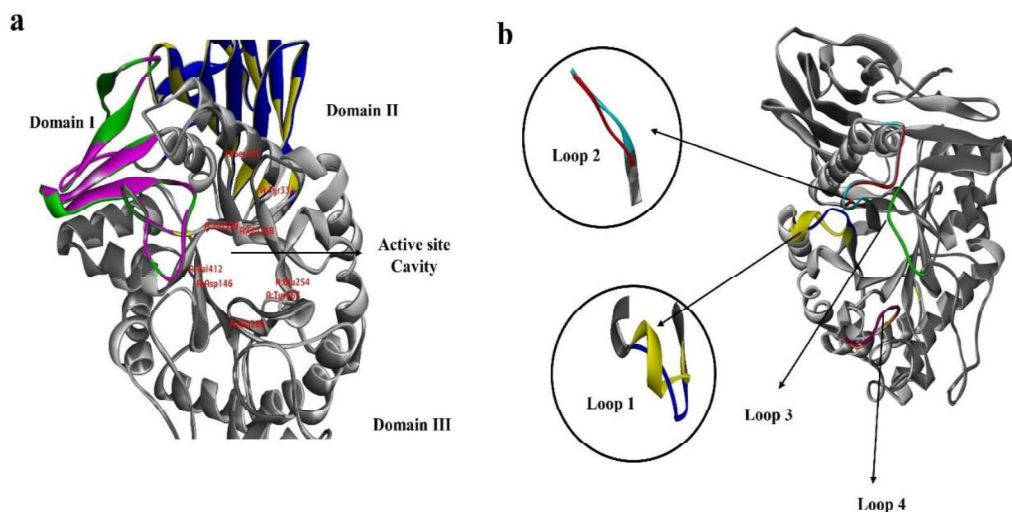


Figure 2.4 (a) Superimposition of rGCCase pH 7.0 domains (I: Green; II: Yellow and III: Light gray) over pH 4.5 rGCCase domains (I: Pink; II: Blue and III: Dark gray) and its active site residues. (b) Superimposition of rGCCase pH 7.0 loops (Loop 1: Yellow; Loop

2: Red; Loop 3: Green and Loop 4: Purple) over pH 4.5 loops (Loop 1: Blue; Loop 2: Turquoise; Loop 3: Pink and Loop 4: Orange) of rGCase. Black circles indicate conformational changes in active site loops 1 and 2.

2.3.3 *In silico* studies

2.3.3.1 Protein and ligand preparation, and grid generation

The grid generated in this study specifically targeted residues surrounding the active site region of rGCase. These residues, which included ARG 139, ASP 146, PHE 147, TRP 198, ASN 253, GLU 254, ALA 257, TYR 263, PHE 265, GLN 266, CYS 267, TYR 331, MET 332, ASP 333, PHE 334, LEU 335, ALA 336, GLU 358, CYS 360, SER 363, LYS 364, PHE 365, TRP 399, ASN 414, PHE 415, and VAL 416, were identified based on their superimposition with the active site residues of hGCase. The active site residues of hGCase were obtained from previously published research papers (Smith, Mullin et al. 2017, Nakagome, Kato et al. 2018). To encompass the active site regions of the proteins, the grid box size was set to dimensions of 54×62×74, with a grid spacing of 0.375 Å. The center of the grid was positioned at coordinates 11.177, -7.564, and 38.121 for the x, y, and z axes, respectively.

2.3.3.2 Docking

The remarkable feature of GCase small molecular chaperones lies in their strong affinity for GCase at the neutral pH environment of the endoplasmic reticulum (ER), followed by dissociation at the acidic pH prevailing within the lysosomes (Beavan and Schapira 2013). In order to examine the specific interaction patterns and assess the binding energies involved, we conducted docking simulations of the AMB (chaperone) with the rGCase protein, which was prepared at two distinct pH values: neutral pH of 7.0 and acidic pH of 4.5. This approach allowed us to gain insights into the nature of their interactions and

quantify the strength of binding between the chaperone and the protein under different pH conditions. The docking results showed interactions with both active and near active site residues of rGCCase in a pH-dependent manner.

For instance, at pH 7.0, AMB interacted with GLU 254 through hydrogen bonding, PHE 265 with π - π stacking, and TRP 399 through π -lone pair. Further, CYS 145, TRP 198, ALA 257, TYR 263, and CYS 267 displayed π -alkyl and alkyl interactions, respectively (**Figure 2.5a-b**).

In contrast at pH 7.0, all interactions with the aforementioned active site residues at pH 4.5 were lost. It interacted with MET 332, PHE 334, and ASP 333 through π -alkyl and H-bonding, respectively (**Figure 2.5c-d**).

AMB interacted to rGCCase tighter at pH 7.0 with the mean binding energy -8.96 ± 0.77 kcal/mol at pH 7.0, which was far better than -6.04 ± 0.77 kcal/mol at pH 4.5. The changes occurring in the binding pattern and binding energy at pH 4.5 were evident in different binding mechanisms.

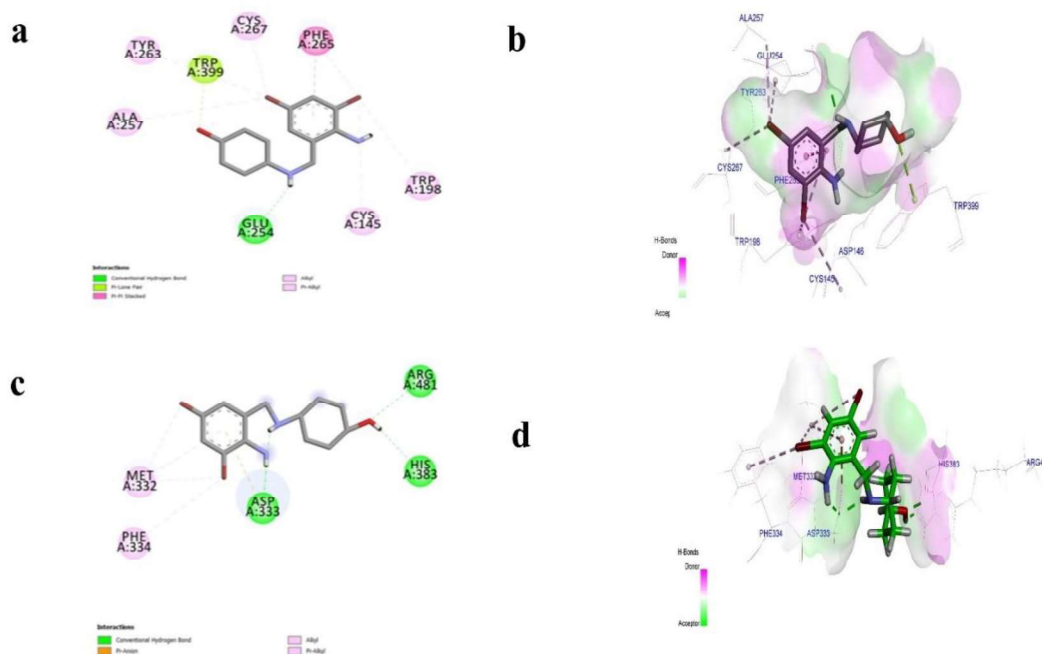


Figure 2.5 2D and 3D docking interactions of the rGCCase-AMB complex at pH 7.0 (a and b) and 4.5 (c and d).

2.3.3.3 Molecular dynamics (MD) simulation

We employed molecular dynamics (MD) simulations to investigate the influence of pH on the dynamic behavior of the protein-ligand complex (Hassan, Shahzadi et al. 2018). Specifically, we conducted pH-dependent MD simulations for the GCCase-AMB complex, considering two pH conditions: neutral (pH 7.0) and acidic (pH 4.5). The simulations were run for a duration of 50 nanoseconds. During the MD simulations, several parameters were calculated to assess the impact of pH on the stability of the GCCase-AMB complex. These parameters included the root mean square deviation (RMSD), which measures the overall structural changes of the complex over time, the root mean square fluctuation (RMSF), which quantifies the local flexibility of residues, the protein-ligand contact time, which indicates the duration of their interaction, the radius of gyration (R_g), which characterizes the compactness of the complex, and the solvent accessible surface

area (SASA), which reflects the extent of surface exposure to the surrounding solvent. By analyzing these parameters, we aimed to gain insights into how pH variations affect the stability and dynamics of the GCCase-AMB complex during the MD simulation.

2.3.3.4 Root mean square deviation

The root mean square deviation (RMSD) is a measure that allows us to assess the average displacement of atoms in a particular frame compared to a reference frame. By calculating the RMSD, we can determine the stability of a protein, as a smaller deviation indicates greater stability. At pH 7.0, an apo form of rGCCase (UBP: unbound protein) and rGCCase-AMB complex (BP: bound protein) displayed mean RMSD values of $1.24 \pm 0.12 \text{ \AA}$ and $1.07 \pm 0.15 \text{ \AA}$, respectively. These data divulged that the AMB bound into rGCCase as the simulation progressed and stabilized it as indicated by lower deviation. However, at pH 4.5, there were no differences in the RMSD values between unbound ($1.43 \pm 0.15 \text{ \AA}$) and bound ($1.46 \pm 0.19 \text{ \AA}$) forms (**Figure 2.6a**). The obtained results indicated that AMB has a weaker binding with the rGCCase at pH 4.5. These results were further confirmed by analyzing the ligand RMSD plot (**Figure 2.6b**) at both pHs. The deviation of AMB was much higher at pH 4.5 ($4.88 \pm 1.28 \text{ \AA}$) than at pH 7.0 ($2.25 \pm 0.24 \text{ \AA}$), indicating that AMB was quite unstable in the acidic medium.

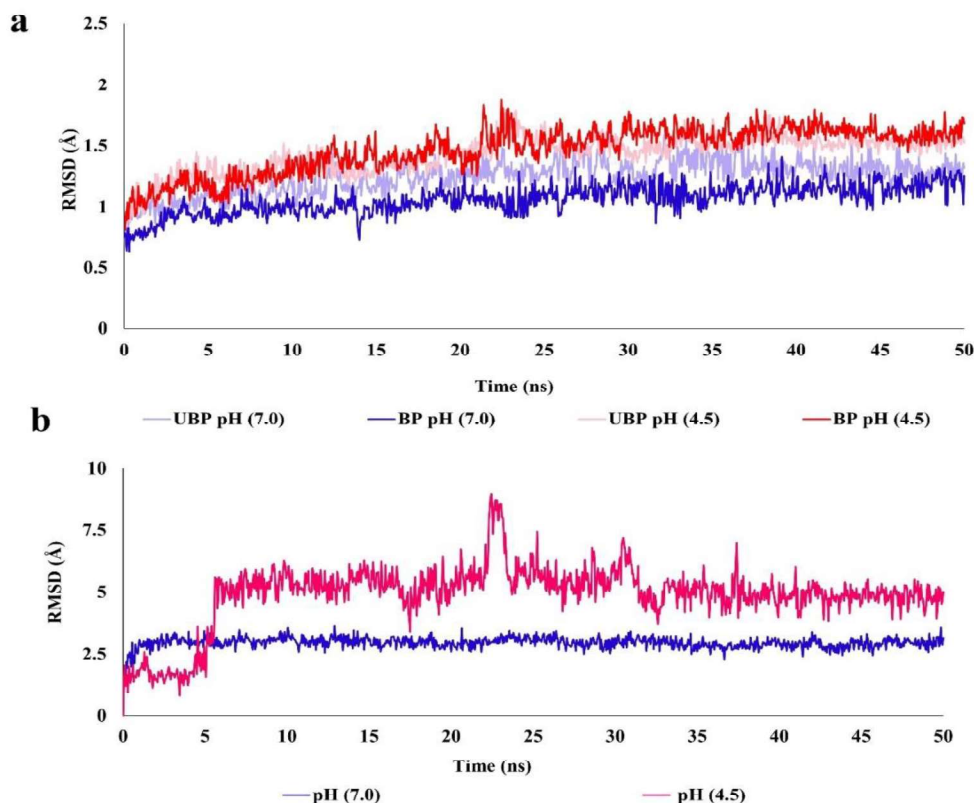


Figure 2.6 RMSD time profiles (a) of the protein C- α atoms in both unbound (UBP: unbound protein) and bound (BP: bound protein) at both pHs (7.0 and 4.5). Ligand RMSD plot (b) at both pHs (7.0 and 4.5).

The change in RMSD values at pH 4.5 might be due to the conformational changes in the loops that cap the active site cavity. Another reason could be the weaker binding interactions between AMB and rGCCase at pH 4.5, as observed in the docking study.

2.3.3.5 Root mean square fluctuation (RMSF) and protein-ligand contact time

RMSF analysis of the rGCCase residues before and after AMB binding indicated the stability of protein residues at both pHs. At pH 7.0, unbound protein displayed higher RMSF compared to AMB bound protein for the residues viz. TRP 198, GLU 254, GLU 358, TRP 399, TYR 331 - ALA 336 (loop 1), VAL 412 – PHE 415 (loop 3), and TYR

263 – CYS 267 (loop 4), as depicted in **Figure 2.7a-b**. Among these, GLU 254 and GLU 358 were catalytic residues present in the active site cavity that were positioned in loop 1- loop 3 regions located at the mouth of the cavity. They all played a crucial role in ligand binding. Similarly, a protein-ligand contact time analysis revealed that the residues *viz.* GLU 358, TYR 263, and GLN 266 have a higher tendency to interact with AMB through hydrogen bonding. These interactions were maintained for 86 – 90 % of the simulation time (**Figure 2.8a and Figure 2.3 in Appendices**). However, TRP 198 and 399 and TYR 331 interacted hydrophobically for approximately half of the simulation time. Also, in the docking study, interactions with TRP 198 and TYR 263 - CYS 267 were due to hydrophobic interactions, and GLU 254 showed hydrogen bonding. These studies confirmed that at pH 7.0, all these interactions were stronger for AMB to make a stable complex with the rGCCase.

At pH 4.5, the RMSF fluctuations of the rGCCase residues of unbound protein and bound protein were similar, indicating the instability of the rGCCase-AMB complex at this pH (**Figure 2.7a and Figure 2.7c**). The protein-ligand contact analysis showed no interactions with the aforementioned residues at this pH (**Figure 2.8b and Figure 2.4 in Appendices**). Similar results were also observed in the docking study. These findings indicated that AMB did not interact with rGCCase active site residues at pH 4.5, contrary to its interactions at pH 7.0. This may be due to conformational changes of the loops found at the entrance of the active site cavity.

We further investigated the RMSF of each atom of AMB. At the pH of 4.5, all atoms, especially cyclohexyl ring (atom number 10 - 17) and the azide moiety (atom number 18) displayed a high degree of fluctuations (mean RMSF; 2.84 ± 0.47) or conformational inflexibility throughout the simulation time than the pH 7.0 (mean RMSF; 0.49 ± 0.05)

These data clearly explained that the AMB was quite unstable at pH 4.5 compared to the neutral pH 7.0 with the higher RMSF values (**Figure 2.8c**).

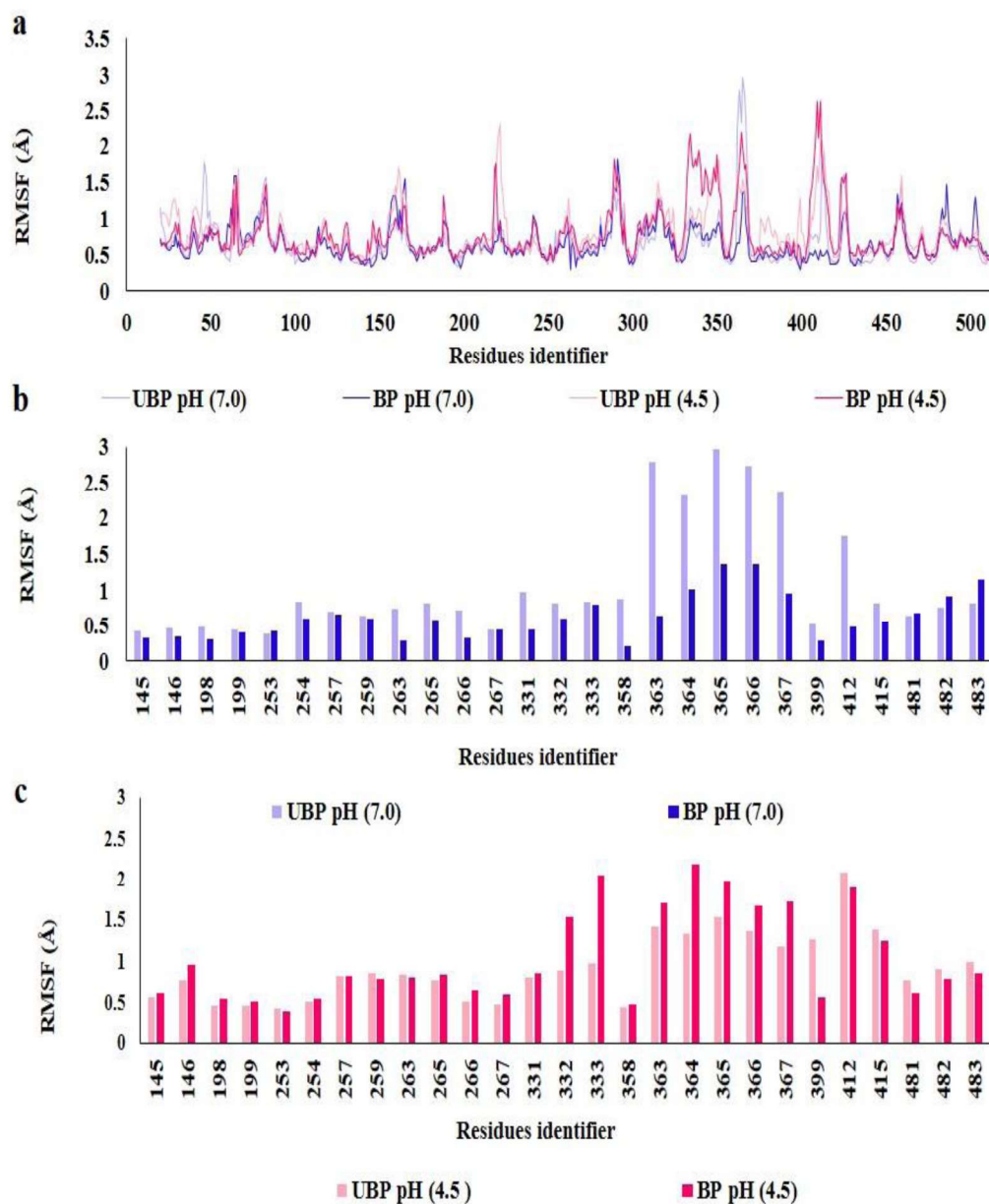


Figure 2.7 RMSF (a, b and c) plots of the protein C- α atoms in both unbound (UBP: unbound protein) and bound (BP: bound protein) form at both pHs (7.0 and 4.5).

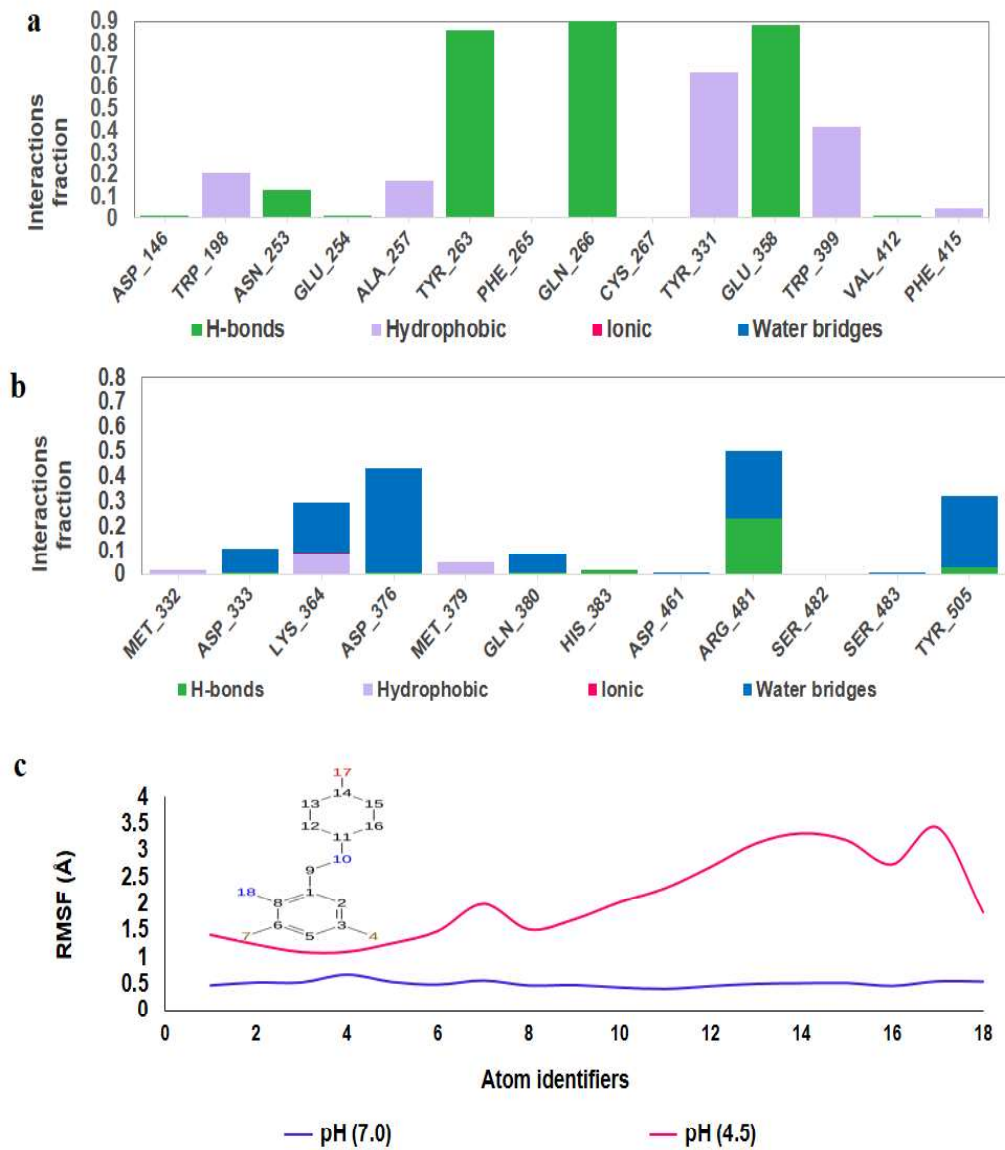


Figure 2.8 Timeline portrayal of the protein-ligand contacts throughout the simulation at pH 7.0 (a) and pH 4.5 (b). Ligand RMSD plot (c) at both pHs (7.0 and 4.5).

2.3.3.6 The radius of gyration (R_g) and solvent accessible surface area (SASA)

The R_g and SASA measure compactness and solvent accessibility *via* MD. Lower R_g or higher compactness is an indicator of higher stability and *vice versa* (Sharma, Tripathi et al. 2019, Ghosh, Chakraborty et al. 2021). R_g 's *versus* time plot of AMB (**Figure 2.9a**) revealed that the AMB at pH 4.5 showed a higher average R_g ($4.043 \pm 0.07 \text{ \AA}$) than the pH 7.0 ($1.27 \pm 0.05 \text{ \AA}$) during the MD. It indicated AMB was stable with a high degree of compactness at pH 7.0 than the pH 4.5 in the protein cavity.

Furthermore, we observed that the change in SASA of AMB with pH in a time-dependent manner (**Figure 2.9b**). SASA is defined as the surface area of the ligand that is accessible to solvent. It was observed that the AMB at pH 4.5 exhibited a higher average SASA ($194.40 \pm 26.65 \text{ \AA}^2$) than the pH 7.0 ($24.29 \pm 4.74 \text{ \AA}^2$), signified a higher magnitude of

instability at pH 4.5 than the pH.

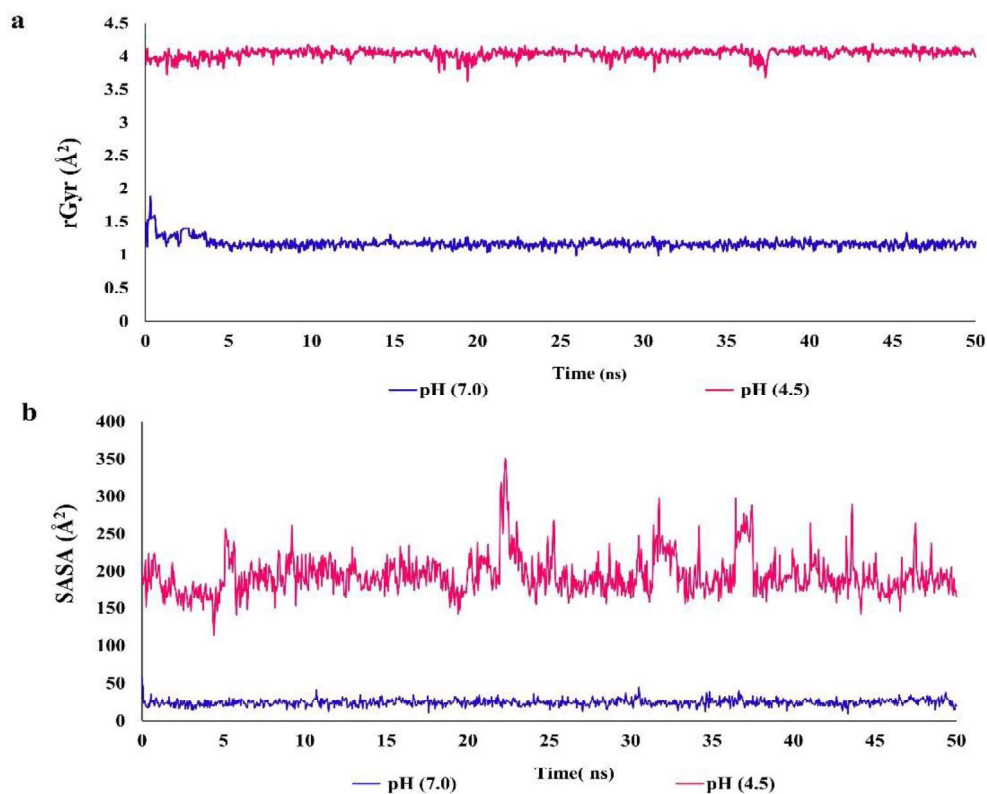


Figure 2.9 Ligand radius of gyration (R_g , 6a) and solvent accessible surface area (SASA, 6b) at both pHs (7.0 and 4.5).

Overall, loss of interactions between rGCCase active site residues and AMB may result in instability of ligand or alteration of the enzyme's structure at pH 4.5. Considering the above findings of the *in silico* studies, we conclude that the AMB showed pH-dependent interactions, which were in higher propensity at the neutral pH than the acidic pH.

2.3.4 Determination of pH-dependent rGCCase enzyme activity profiles in the presence of chaperone

2.3.4.1 pH-dependent IC₅₀ measurement

In silico studies confirmed that the strength of the interactions pattern of AMB was highly pH-dependent; the best was at pH 7.0 and least at pH 4.5. Therefore, we have developed an *in vitro* model for rGCCase and investigated the activity of the AMB from pH 7.0 to 4.5. Consistent with *in silico* studies, the inhibitory activity (IC₅₀) of the AMB at pH 7.0 was found to be 8.2 ± 2.6 μ M; however, the tendency of inhibiting enzymes became weaker after the pH was decreased. Compared to the IC₅₀ value at pH 7.0, its IC₅₀ value significantly increased by 6-fold and 62.3-fold at pH 5.5 and 5.2, respectively (**Figure 2.10 and Table 2.3**). Unexpectedly, AMB showed non-inhibitory effects on rGCCase in acidic environments in the range of pH 5.0-4.5, even up to 1.5 mM concentration. The loss in the inhibitory activity at the acidic pH could be due to the ligand instability or loss of rGCCase-AMB interactions and contact times with the active site residues of rGCCase, as observed in our MD simulation.

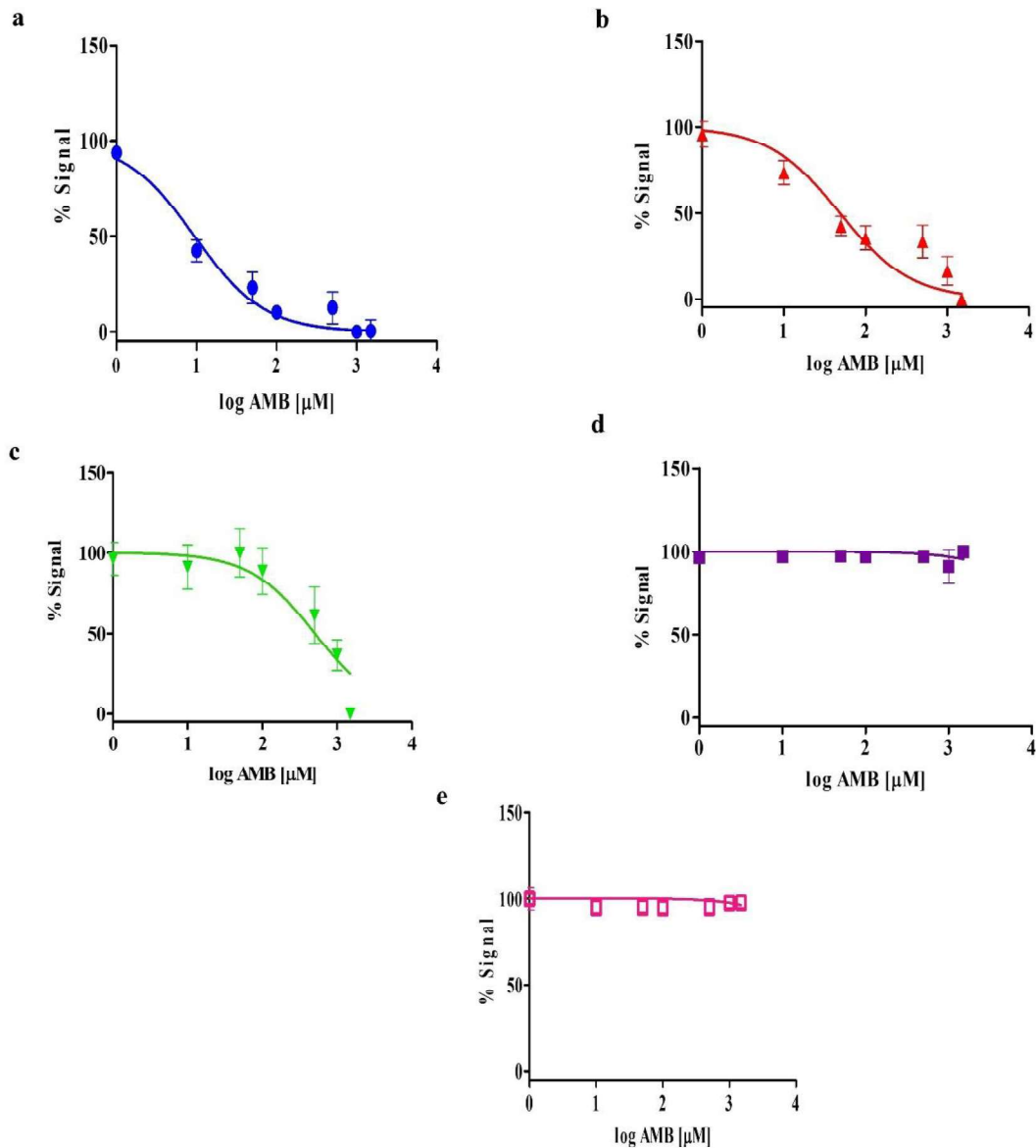


Figure 2.10 Graphical representation of the concentrations and pH response profiles of AMB for rGCCase. Inhibitory effect of the AMB against rGCCase activity at pH 7.0 (a), pH 5.5 (b), pH 5.2 (c), pH 5.0 (d) and pH 4.5 (e). rGCCase activity shown in terms of % fluorescent signal.

Table 2.3 Statistical representation of the pH-dependent IC₅₀ profiles of AMB for rGCCase

pH	IC ₅₀ (μM)	R ²
pH 7.0	8.2 ± 2.6	0.94
pH 5.5	48.2 ± 6.4 ^a	0.86
pH 5.2	510 ± 78 ^{a, b}	0.70
pH 5.0	NI (1500) *	0
pH 4.5	NI (1500) *	0

IC₅₀ values are shown in the form of mean ± SD (n=3). p < 0.05 are considered to be significant. ^ap < 0.05 compared to pH 7.0 and ^bp < 0.05 compared to pH 5.5 [One-way ANOVA followed by Tukey test. *NI, non-inhibitory effect (highest concentration tested, μM, micromolar).

2.3.4.2 pH-dependent residual activity assay

GCCase chaperons are pH-dependent enzyme inhibitors, exposed to broad ranges of pHs (from the ER pH 7.0 to the lysosomal pH 4.5) during their trafficking (Bendikov-Bar, Maor et al. 2013). Therefore, it is hard to balance its functional inhibition in the ER against residual activity found in the lysosomes. AMB bound best and inhibited more to rGCCase at pH 7.0. Thus, we have chosen 0.5-2.0-fold concentration of near to IC₅₀ value of pH 7.0 and changed pHs according to the enzyme trafficking (pH 7.0-pH 4.5) to investigate their remaining enzyme activity after inhibition by AMB in terms of residual activity (**Figure 2.11**). At pH 7.0, the residual activity was found to be 47.43 ± 12.18 % and 42.17 ± 14.27 % for 10 and 20 μM of AMB, respectively; however, these activities

dramatically rose with fallen pHs corresponding to the same pH control group. At the same concentration, unexpectedly, its residual activity was reached about $99.66 \pm 18.57\%$ and $99.24 \pm 10.82\%$ at pH 4.5. This non-inhibitory effect of AMB in the acidic medium might be due to instability of AMB or structural changes of the active site loops, which was clearly shown in *in silico* study.

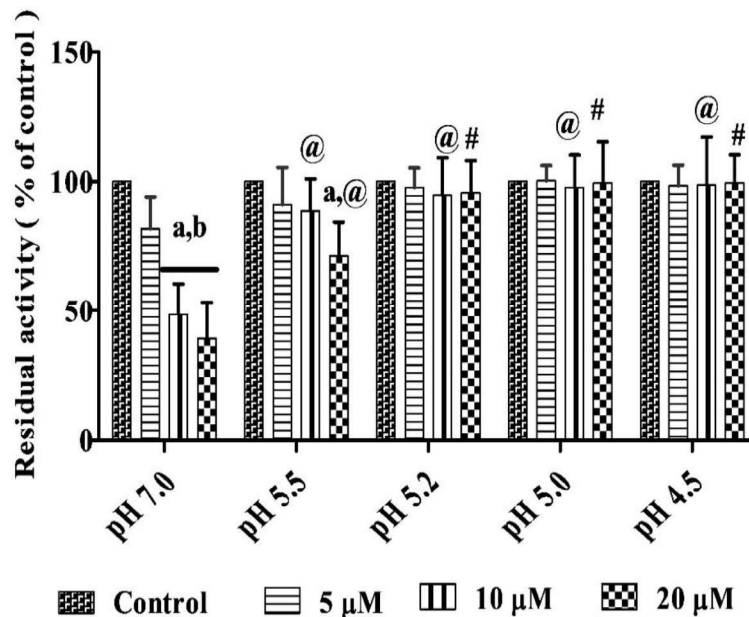


Figure 2.11 pH-dependent rGCCase residual activity profiles in the presence or absence of ambroxol (AMB). All values are expressed in the form of mean \pm SD; $n = 3$. ^a $p < 0.05$ compared to control (0 μ M, without AMB), ^b $p < 0.05$ compared to 5 μ M, [@] $p < 0.05$ compared to pH 7.0 and, [#] $p < 0.05$ compared to both 7.0 and pH 5.5 [Two-way ANOVA followed by Bonferroni multiple comparison test, Graph Pad Prism 5.1 Software, Inc.).]

Moreover, obtained results confirmed that these sub-inhibitory concentrations of AMB inhibited the enzyme functionally at the ER pH (neutral) but did not alter the enzyme's activity when kept on lysosomal pH (acidic). Thus, we can further use these concentrations to optimize the dosage regimen to balance the overall enzyme activity.

Furthermore, this *in vitro* study is consistent with an antecedent study that documented chaperones bind to GCCase tighter at the ER pH than the lysosomal pH (Yu, Sawkar et al. 2007, Zheng, Chen et al. 2016).

2.3.4.3 pH-dependent enzyme kinetics assay

A pH-dependent kinetics study was performed to examine whether AMB altered the mode of GCCase inhibition during their trafficking from the pH 7.0 to 4.5. For this objective, we have selected only those pHs at which AMB showed inhibitory activity, that was pH 7.0, 5.5, and 5.2. The Michaelis-Menten curves (**Figure 2.12a-9c**) were plotted at each pH between velocity *versus* substrate concentration to extract the V_{max} and K_m . Results illustrated that an increase in the amount of AMB increased in their slope (decreased V_{max}) and intercepts (higher K_m); hence it presented a mixed-model of inhibition at all given pHs (**Figure 2.12d-9f**). This model suggested that AMB acts on both free enzyme and enzyme-substrate complex.

Meanwhile, AMB binding affinity at pH 7.0, pH 5.5, and pH 5.2 were calculated in terms of K_i (inhibition constant) by Dixon plot (replots the slopes of reciprocal velocity *versus* inhibitor concentrations, **Figure 2.12g-9i**). Higher the K_i value, the lower the affinity of the inhibitor for the enzyme. At pH 7.0, AMB gave a constant inhibition value, K_i , $4.3 \pm 1.2 \mu\text{M}$ (**Figure 2.12g**) for the rGCCase. However, compared to it, this value was increased by 6-fold ($25.7 \pm 3.4 \mu\text{M}$) and 70.6 - fold ($303.5 \pm 56.8 \mu\text{M}$) for pH 5.5 (**Figure 2.12h**) and 5.2 (**Figure 2.12i**), respectively, signifying that AMB's affinity for the rGCCase dropped out persistently during shifting pH from 7.0 to 5.2. As we observed in MD studies, loss of protein-ligand contact time, AMB instability, and change in the rGCCase active site loops could be the possible reasons for losing affinity while shifting the pH from neutral to acidic.

Exploring wild-type rat glucocerebrosidase: Insights into chaperone interactions and mechanism through *in silico* and *in vitro* studies

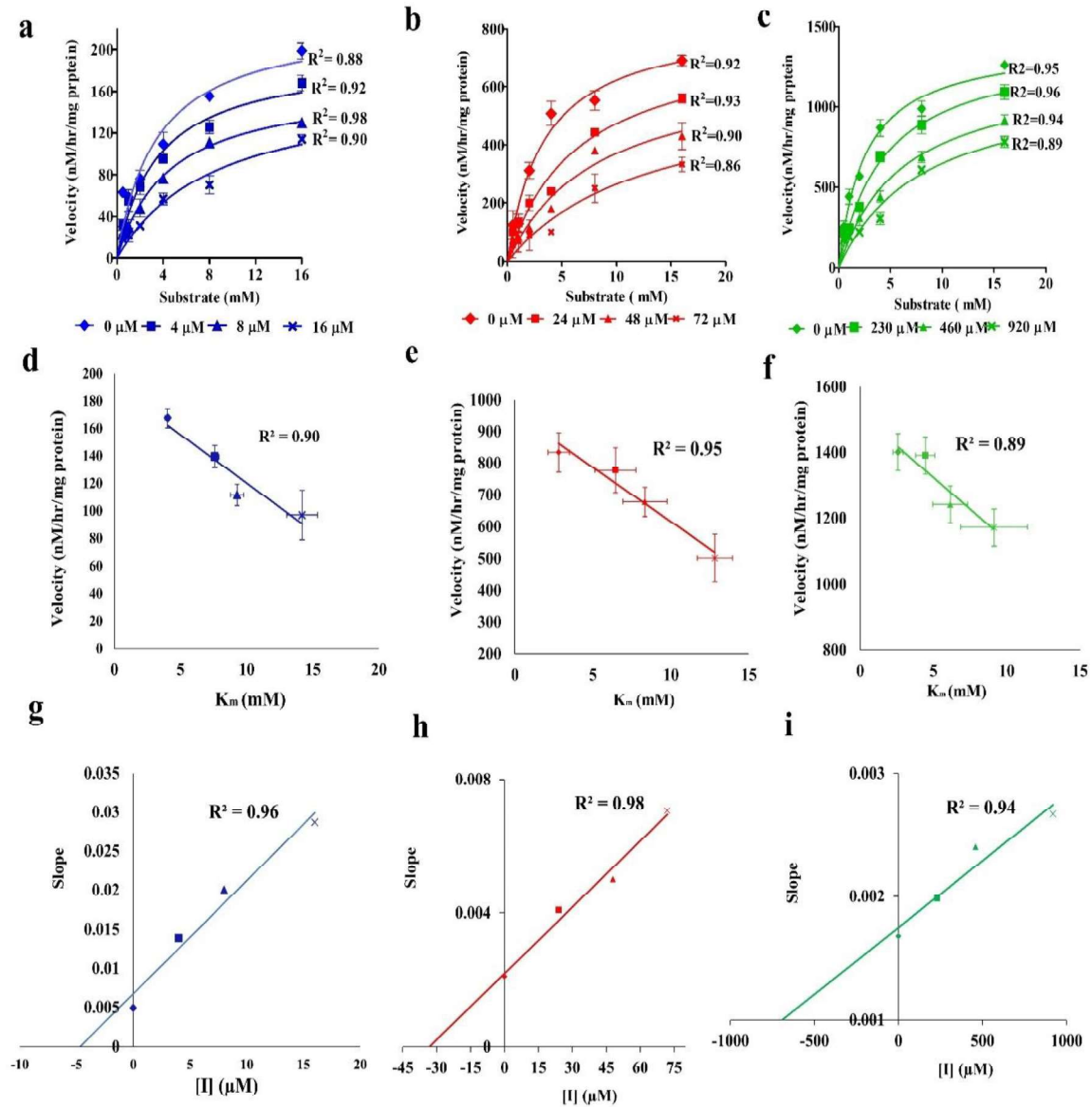


Figure 2.12 Blue, red, and green plots show AMB mode of rGCase inhibition mechanism at pH 7.0, pH 5.5, and pH 5.2, respectively. The Michaelis-Menten curves are illustrated in a, b, and c. Plots of K_m versus V_{max} show in d, e, and f. Dixon plots depict in g, h, and i. All values are shown as mean \pm SD [Non-linear regression analysis, Graph Pad Prism 5.1 Software, Inc.]

2.3.4.4 Thermal denaturation assay (TDA)

To assess the stability of rGCCase and its chaperoning effect of AMB, we employed the TDA (thermal denaturation assay) method. In this method, we denatured the enzyme by exposure to heat, both in the presence and absence of AMB, and measured the enzyme activity relative to unheated in terms of stability (**Figure 2.13**). The untreated group significantly lost the enzymatic activity after exposure to heat in a time-dependent manner. The maximum loss of the rGCCase activity with only $14\% \pm 2.9\%$ remaining was found after 60 min of heating. However, when AMB was added in varying concentrations, the reduction in enzyme activity was significantly attenuated in a concentration-dependent manner. AMB treated with 25 μM concentration significantly failed to retain GCCase activity after 40 min of heating, compared to that corresponding time of the untreated group. While 50 and 100 μM concentrations tended to protect the GCCase from thermal denaturation and retained ~2–3-fold much activity at all-time points compared to that corresponding time of the untreated group. The reason for the enzyme activity retained by AMB could be due to it bound and stabilized rGCCase prior to denaturation. The binding of AMB in order to stabilize rGCCase reflects its chaperoning characteristic. This observation was implicit with our above *in silico* studies showing AMB stabilized rGCCase protein by interacting with its active site residues.

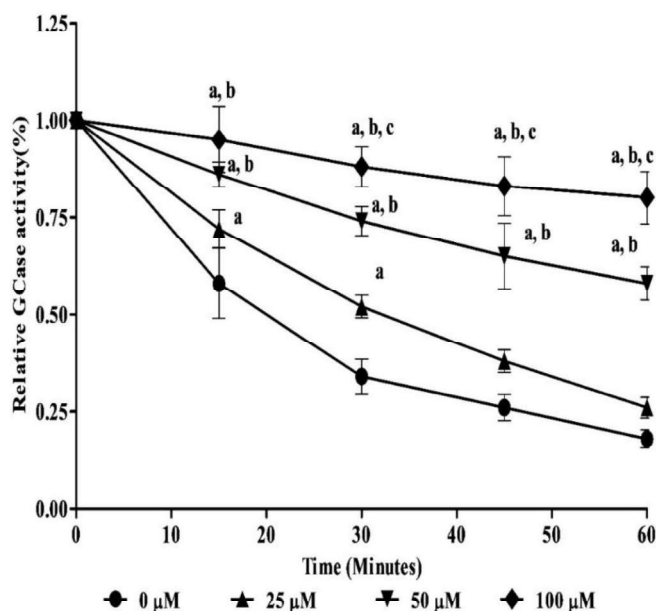


Figure 2.13 Stabilization of rGCase by AMB through heat inactivation method. All values are mean \pm SD; n = 3. ^ap < 0.05 compared to corresponding time of untreated group, ^bp < 0.05 compared to that corresponding time of 25 μ M, ^cp < 0.05 compared to the corresponding time of 50 μ M [Two-way ANOVA followed by Bonferroni multiple comparison test, Graph Pad Prism 5.1 Software, Inc.].

2.4 Conclusion

Conclusively, these studies give the 3D-structural insight of the rGCase and contributed to understanding the interactions between rGCase and chaperone and its mechanism. Homology models were used to predict 3D models of apo rGCase at neutral and acidic pH. pH-dependent docking and MD simulation studies revealed that chaperone (AMB) made a stable complex with rGCase residues TRP 198, TYR 263, GLN 266, TYR 331, GLU 358, and TRP 399 at the ER pH 7.0 than at lysosomal acidic pH 4.5. Consistent with *in silico* studies, *in vitro* studies showed higher inhibitory activity and binding affinity at pH 7.0 than pH 4.5. Moreover, AMB was identified as a potent rGCase

stabilizer that binds and stabilizes rGCCase prior to denaturation. All these properties led to the emergence of the AMB as a potential chaperone for the rGCCase. This study would facilitate designing and screening of chaperones at an early stage of drug discovery to improve the treatment strategies of PD. This can be an effective screening method for the evaluations of chaperones for new drug discovery.

2.5 Summary

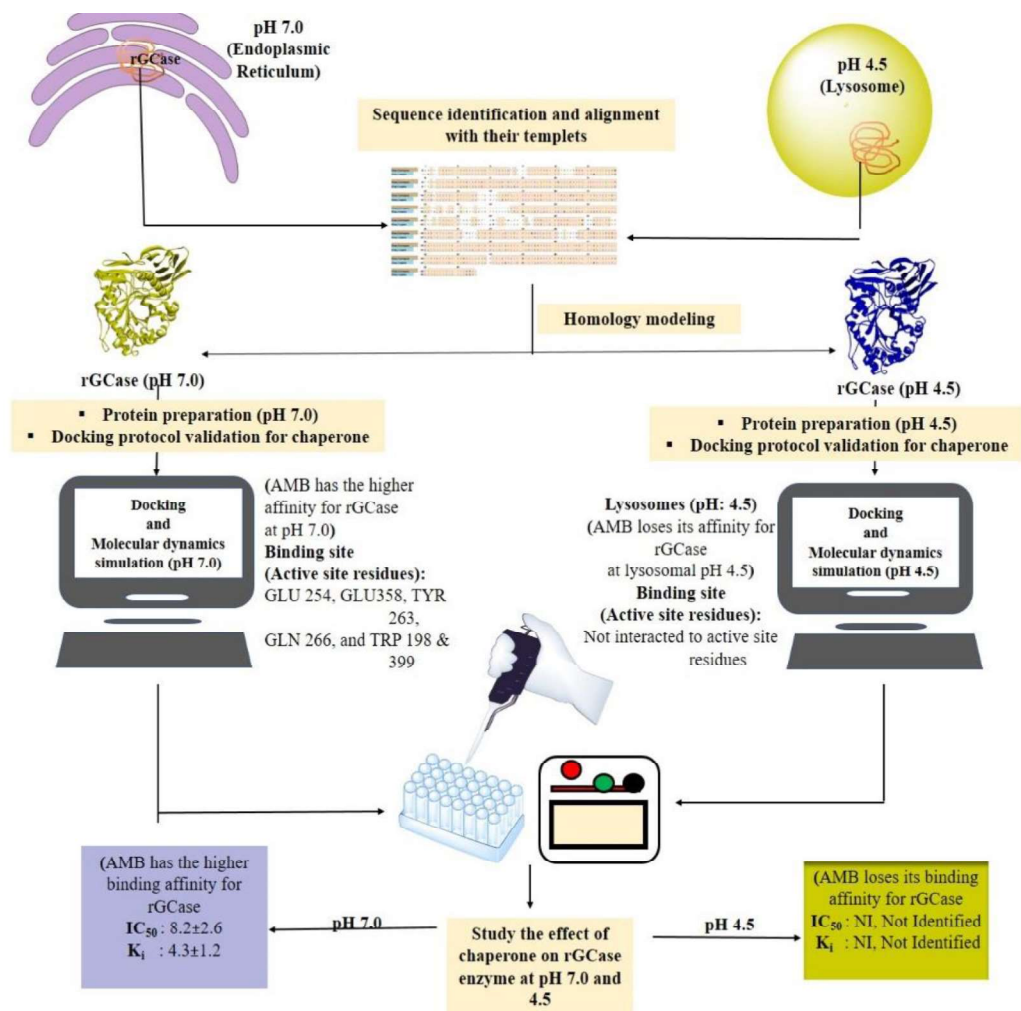


Figure 2.14 summarises the outcomes of the objective 1

- The study provides structural insight into rGCCase and its mechanism of interactions with chaperone.
- Residues TYR 263, GLN 266, TYR 331, and GLU 358 play a major role in rGCCase-chaperone interactions.

- Chaperone shows stronger inhibitory activity and binding affinity for rGCCase at pH 7.0 than pH 4.5.
- AMB acted as a potent rGCCase stabilizer, which improved rGCCase thermostability.
